ELSEVIER

Journal of Nuclear Materials 241–243 (1997) 745–749

journal of nuclear materials

Strong toroidal asymmetries in power deposition on divertor and first wall components during LHCD on TdeV and Tore Supra

J. Mailloux [a,*,1], Y. Demers [a,2], V. Fuchs [a,3], M. Goniche, P. Jacquet [a,1], C. Boucher [a,1], A. Côté [a,3], C. Côté [a,4], J. Gunn [a,1], B. Terreault [a,1,b], P. Bibet [b], P. Froissard [b], D. Guilhem [b], J.H. Harris [b,5], G. Rey [b], M. Tareb [b]

[a] *Centre canadien de fusion magnétique, 1804 Boulevard Lionel-Boulet, Varennes, Qué., Canada J3X 1S1*
[b] *Centre d'études de Cadarache, Association Euratom-CEA, 13108 St. Paul-les-Durance, France*

Abstract

Strong toroidal asymmetries in power deposition during lower hybrid current drive experiments have been observed on TdeV and Tore Supra. These asymmetries are characterized by high heat loads on components magnetically connected to the LHCD antenna. The experimental results indicate that fast electrons generated by the rf fields in the scrape-off layer in front of the antenna are responsible for the localized heat loads. The rf power lost in the edge through this channel increases with both the edge density and the rf power level. In TdeV, the fraction of the injected power lost can exceed 10% at high power and high density, while it stays under 2% in Tore Supra. A simple model describing the trajectories of electrons in front of the antenna suggests that the high $N_{\|}$ components of the near field spectrum are responsible for the acceleration of the scrape-off layer electrons.

Keywords: TdeV; SOL plasma; Energy deposition; Rf heating

1. Introduction

During lower hybrid current drive (LHCD) experiments on ASDEX [1], Tore Supra [2] and TdeV [3], large toroidal asymmetries in the power deposition have been observed. Components magnetically connected to the LHCD antennas were subject to high and localized heat loads. These high heat loads are detrimental to LHCD performance as they have been shown to lead to hot spots and large impurity influxes. The first section of this paper gives a description of the toroidal asymmetries observed with LHCD on TdeV. This same topic on Tore Supra has already been reported in [2,4]. The experimental characterization of the phenomena in both machines is presented in the following section. The last section presents a simple model showing how cold electrons can be accelerated by the time and space varying electric near field of a LHCD antenna.

2. Toroidal asymmetries in power deposition in TdeV

TdeV is a divertor tokamak with major and minor radii of 0.87 and 0.25 m respectively. In the experiments described below, it was operated in an upper single null configuration, with 140 kA $\leq I_p \leq$ 190 kA and 1.4 T $\leq B_T \leq$ 1.8 T. The LHCD system operates at 3.7 GHz and its multijunction antenna generates a spectrum with $N_{\|0}$ adjustable between 2.0 and 3.3. The main diagnostic used to characterize the localized heat loads consists of more than

* Corresponding author. Tel.: +1-514 652 8879; fax: +1-514 652 8625; e-mail: mailloux@ccfm.ireq.ca.
[1] INRS-Énergie et Matériaux, Varennes, Québec, Canada.
[2] MPB Technologies Inc., Dorval, Québec, Canada.
[3] Hydro-Québec, Varennes, Québec, Canada.
[4] Consultants ProTek, Brossard, Québec, Canada.
[5] Oak Ridge National Laboratory, Oak Ridge, USA.

PII S0022-3115(96)00598-3

60 thermocouples installed in divertor plates and limiters, at several poloidal and toroidal locations. Fig. 1 is a poloidal view of TdeV showing the magnetic field lines from a typical calculated equilibrium. It should be noted that the outer magnetic separatrix strikes the horizontal divertor plates while the inclined divertor plates intercept a large part of the SOL. In most of the experiments described below, the directions of B_T and I_p were such that the connection along the magnetic field lines from the antenna mouth was to the inclined divertor plates in the ion drift direction, and to the inner divertor components in the electron drift direction.

Fig. 2 shows the energy deposited with and without LHCD on the inclined divertor plates as a function of their toroidal location. With Ohmic heating only, the toroidal distribution is fairly symmetrical (Fig. 2a). When LHCD is used, the energy deposited on all the plates increases as expected, but large asymmetries develop with some of the plates receiving as much as 10 times more energy than the others (Fig. 2b, c). The plates receiving the heaviest load are those that are magnetically connected to the LHCD antenna mouth. When the safety factor q_a is changed, the location of the highest power load follows the surface magnetically connected to the antenna mouth. High power loads were also observed on the components magnetically connected to the antenna in the electron drift direction, and experiments with B_T and/or I_p reversed indicated that the energy deposited on components connected to the antenna mouth from either direction is of the same magnitude.

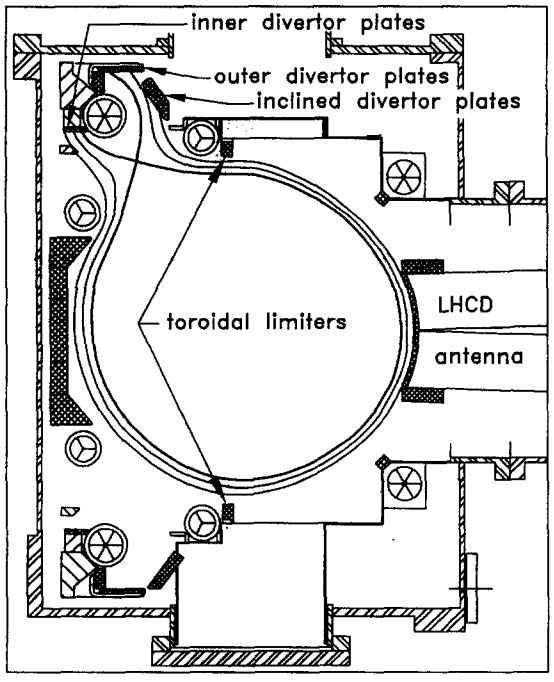

Fig. 1. Poloidal view of TdeV showing the positions of the plates and limiters instrumented with thermocouples, and the LHCD antenna.

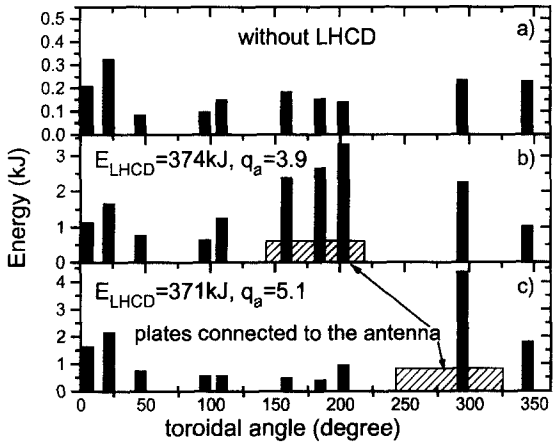

Fig. 2. Toroidal distribution of the energy deposited on the inclined divertor plates (only plates instrumented with thermocouples are shown), for (a) Ohmic heating only, (b) and (c), LHCD + Ohmic heating, $P_{LHCD} = 550$ kW, $\bar{n}_e = 2.4 \times 10^{19}$ m^{-3}.

The localized high power loads are not due to the suprathermalelectrons created in the central plasma and diffusing out. In fact, as the suprathermal electrons reach the plasma edge, they are rapidly transported to the horizontal divertor plates, where they deposit their energy very close to the separatrix strike point. Moreover, they are symmetrically distributed toroidally. The measurements indicate rather that a sizeable fraction of the rf power is dissipated directly in a thin plasma layer of ~ 1 cm just in front of the antenna and that the fast particles created there follow the open field lines to the plates or limiters, causing the asymmetries in energy deposition. Note that the TdeV antenna guard limiters do not intercept a large fraction of the accelerated particles because they are flush mounted on the grill mouth.

3. Experimental characterization

3.1. Dependence on P_{LHCD}, n_e and $N_{\|0}$

On Tore Supra ($R = 2.37$ m, $a = 0.80$ m, $I_p = 1.7$ MA), localized heat fluxes are also observed on the antenna guard limiters and first wall components magnetically connected to the antenna rows, and specific experiments were carried out to investigate their dependence on P_{LHCD}. The LHCD system operates at the same frequency and uses the same type of multijunction antenna as TdeV, however with $N_{\|0}$ between 1.4 and 2.4. Although the launched power is much higher on Tore Supra, up to 6 MW for two antennas, the power densities, and consequently the electric fields, are of the same order of magnitude for the two machines.

The experiments were conducted in the limiter configuration, with the plasma leaning on the inner wall. The antennas were set 4 cm behind the LCFS and one of the outboard vertical limiters was pushed 2.5 cm from the plasma. In this configuration, for a specific value of plasma current ($I_p = 0.95$ MA, $q_a = 6.0$), antenna 2 is magnetically connected to this limiter in the ion-drift direction, with a connection length $L_{||} = 15$ m. The power dissipated in front of the grill is intercepted in part by this vertical limiter, but also by the antenna guard limiters, because they are protruding 2 mm in the radial direction. The heat flux on the limiters were calculated in the semi-infinite wall approximation using the surface temperatures measured by IR imaging. Fig. 3 shows that the heat fluxes increase with the power launched by antenna 2 and the shape of the curves suggests that the dissipation phenomenon is not linear. However, it is not clear whether this non-linearity is inherent to the power dissipation process or if it is due to variations of plasma parameters in front of the grill with P_{LHCD}. Similar non-linearities with LHCD power have been observed on TdeV.

The dependence on the density was investigated on TdeV. Fig. 4shows the fraction of P_{LHCD} lost on the inclined plates, F_{loss}, due to rf dissipation in the edge as a function of the density at the grill mouth. In these shots, the antenna-separatrix distance is ~ 1.5 cm, $q_a = 3.9$, the connection length between the antenna mouth and the inclined plates is ~ 10 m in the ion drift direction, and the reflection coefficient is in the range of 6 to 12%. The spatial average of the electric field amplitude at the mouth of the grill is in the range of 3.2×10^5 to 3.5×10^5 V/m. The highest values of the electric field generally correspond to low density shots which have higher reflection coefficients. The density at the grill, $n_{e,grill}$ was measured with a Langmuir probe located in the guard limiter of the antenna and it was varied by changing the line average density in the range of 2 to 6×10^{19} m^{-3}. As can be seen, F_{loss} is well correlated with the density at the grill. The correlation with $\tilde{n}_e$ (not shown) is not as good indicating that the edge plasma density is, as expected, a more relevant scaling parameter. At high density, F_{loss} is more than 10%, implying that the total loss could be $\sim 20\%$ of P_{LHCD} if one takes also into account the losses in the electron drift direction. It should be noted that on TdeV good coupling is achieved for densities at the grill in the lower range of Fig. 4. During normal operation, the density at the grill is maintained in this range by adjusting the antenna-separatrix distance.

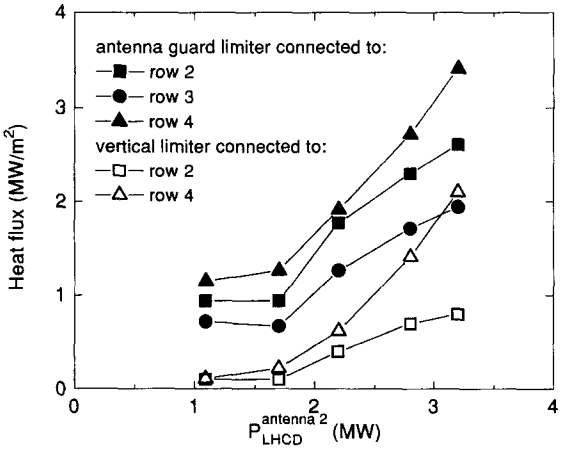

Fig. 3. Heat fluxes on the antenna guard limiters and vertical limiter magnetically connected to antenna 2 of Tore Supra as a function of LHCD power, $\tilde{n}_e = 2.6 \times 10^{19}$ m^{-3}, $3.0 \leq R \leq 4.9\%$.

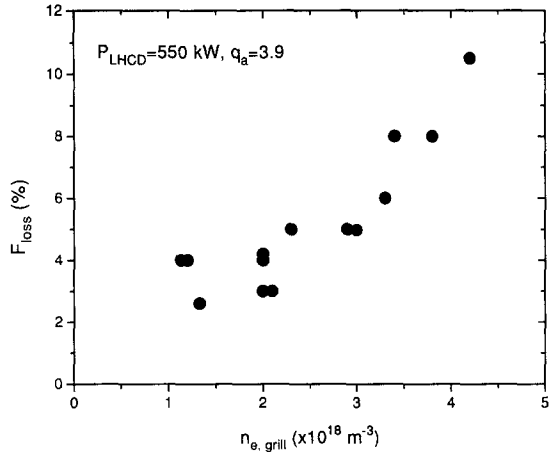

Fig. 4. Fraction of P_{LHCD} lost on the inclined plates on TdeV (F_{loss}) as a function of the density at the grill.

On Tore Supra, when the line average density was changed from 1.6 to 3.6×10^{19} m^{-3}, the heat fluxes on the antenna guard limiters were almost unchanged. However, the weak decrease in the reflection coefficient, from 4.8 to 4.1%, indicates that the density at the antenna mouth had not varied by much and most likely stayed in the lower range of Fig. 4. The total power lost on the antenna guard limiters and on the vertical limiter of Tore Supra was estimated from the thermographic data and from calorimetric measurements of the water-cooled vertical limiter. For all the shots considered, it lies between 1 and 2% of the launched power, which is about 2 times lower than the lowest value measured on TdeV.

The variation with $N_{||0}$ was also investigated. On TdeV, within experimental errors ($\sim 20\%$), no dependence of F_{loss} on $N_{||0}$ was observed in the range of $2.0 \leq N_{||0} \leq 3.3$. On Tore Supra, the IR imaging of antenna 2 guard limiters shows that the heat load for $N_{||0} = 1.6$ is lower than for $N_{||0} = 2.4$. However, antenna coupling calculations with SWAN [5] for $N_{||0} = 1.6$ show that a decrease of the rf field at the antenna mouth could be responsible for the heat load reduction.

3.2. Type and energy range of the accelerated particles

Although it was not possible to measure directly which particles, electrons or ions, are accelerated by the rf field in front of the antenna, a number of experimental observations lead us to conclude that they are electrons. One of these is that the heat load patterns on the antennas of both machines are those corresponding to passing particles. Accelerated ions would be expected to be deeply trapped in banana orbits and ripple wells as they would be heated preferentially in the perpendicular direction by the rf field.

The lower and upper energy limits of the fast electrons have been estimated on TdeV. The lower limit comes from measurements done with a Langmuir probe situated in the SOL and magnetically connected to the antenna. The probe was damaged by the high power density flowing in the SOL, but the heat flux deduced from its I–V characteristics was significantly below damage threshold. This indicates that non-Maxwellian electrons with $E > \sim 200$ eV are responsible for most of the deposited heat load [6]. It should be noted that fast electrons are likely to change the sheath transmission factor, but that effect was neglected in the calculation of the fraction of P_{LHCD} dissipated in the SOL. The upper energy limit was provided by the soft X-ray detector array, whose detection range is 5 keV to 20 keV, for thick target bremsstrahlung. Since it measured no emission from the inclined plates bombarded by the fast electrons, the upper energy limit is estimated to be 5 keV.

4. Model and discussion

Mechanisms responsible for localized heating and particle acceleration in the vicinity of ICRH antennas have been studied extensively and are fairly well understood [7]. However, because of the difference in frequency and wavenumber spectrum, they cannot satisfactorily explain the experimental observations made during LHCD on Tore Supra and TdeV. A more promising approach [8] is to study the dynamics of electrons in the rf fields at the grill mouth. A simple model neglecting plasma effects and including only the component of the rf electric field parallel to B_{T} was used to calculate the trajectories of electrons in front of the TdeV grill. The equation of motion is:

$$\mathrm{d}^2z/\mathrm{d}t^2 = (q_e/m_e)E(z, t) \qquad (1)$$

where q_e and m_e are the electronic charge and mass, and $E(z, t)$ is the electric field at the grill–plasma interfacecalculated with the SWAN code, for typical coupling parameters of TdeV, $P_{\mathrm{LHCD}} = 550$ kW (275 kW per row), reflection coefficient = 7% and $N_{\|0} = 3.3$ (Fig. 5a). Eq. (1) was numerically integrated to obtain the velocity of the electrons at the exit of the grill, $z = L$. Calculations were made for a 20 eV Maxwellian distribution of 2500 electrons, with initial position $z = 0$ and a random phase at the entry of the grill. Fig. 6 shows the distribution of the final energy of the electrons when they exit the grill, compared with the distribution of the initial energy. The final distribution is wider, with a long tail at high energy, showing that most of the electrons have gained energy from the field. The mean final energy of the electron sample is 320 eV and its maximum energy is 2.2 keV, which corresponds well to the energy range obtained from the measurements (Section 3.2). The calculations also show that the acceleration does not depend strongly on the current drive direction, as similar results are found for electrons entering the grill at $z = L$.

The acceleration of electrons in a field which vanishes on the average in space and time can be understood as follows. The electric field at the grill mouth can be represented by a superposition of travelling waves with different $N_{\|}$ values. Fig. 5b shows the $N_{\|}$ spectrum of the electric field used for the calculations described above. In addition to the lowest $N_{\|}$ component, which interacts with

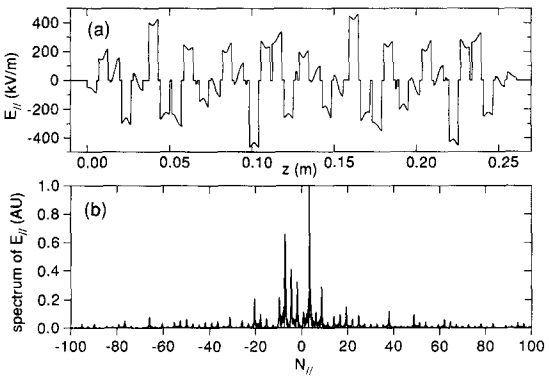

Fig. 5. (a) Spatial structure of the electric field at the TdeV grill mouth, at a fixed time, (b) $N_{\|}$ spectrum of the electric field shown in (a).

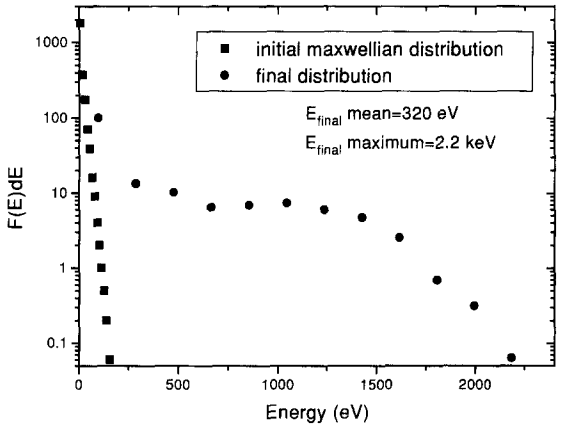

Fig. 6. Energy distribution of the electrons before (■) and after (●) acceleration by the antenna electric field.

the electrons near the plasma centre, there are peaks at much higher values of $N_{||}$ with non negligible intensity. They correspond to small parallel wavelengths (for $|N_{||}| > 50$, $\lambda_{||} > \sim 1.5$ mm) and are due to small scale length features of the grill such as the septum thickness, edge shapes, etc. For $|N_{||}| > \sim 50$, the waves have a phase velocity low enough to interact through Landau damping with thermal electrons in front of the grill. Acceleration up to ~ 2 keV, which corresponds to interaction with lobes at $|N_{||}| \sim 10$, is possible because the field intensity in front of the grill is large enough for the high $N_{||}$ modes to form an overlapping system of resonances [9,10].

Given the fact that the high $N_{||}$ part of the spectrum does not change appreciably with the antenna phasing, the model correctly predicts that the acceleration will not depend strongly on $N_{||0}$. However, additional work is needed to explain the parametric dependencies on n_e and P_{LHCD}. A more complete model that includes self consistently both plasma and wave propagation effects might be required.

Two approaches to reduce the fraction of the rf power lost in the SOL are currently under study. The first one is to reduce from the outset the available power in the high $N_{||}$ part of the spectrum by modifying the small scale length features of the antenna. Secondly, since the high $N_{||}$ components are highly evanescent in a plasma below the cut-off density, the fraction of power at high $N_{||}$ that would reach a region of sufficiently high density for efficient damping could be reduced by controlling the edge plasma parameters, and in particular the thickness of the vacuum gap in front of the grill. However, this means that a compromise between low power dissipation and good coupling would have to be found. Finally, it should be noted that the strong dependence on n_e observed experimentally implies that power dissipation in the SOL is a more serious problem for antennas operating at higher $N_{||0}$ since the optimal coupling density increases with $N_{||0}^2$ ($n_e \approx n_{e,\text{cut-off}} N_{||0}^2$).

Acknowledgements

The authors wish to thank T.E. Evans for helpful discussions. We are indebted to the staff of TdeV and Tore Supra for the operation of the machines and LHCD systems. The Centre Canadien de Fusion Magnétique is supported by the government of Canada, Hydro-Québec, and INRS.

References

[1] T.E. Evans et al., J. Nucl. Mater. 176–177 (1990) 202.
[2] M. Goniche et al., Proc. 21th EPS Conf. Plasma Phys. 17c (1994) III-1042.
[3] J. Mailloux et al., APS Bull. 40 (1995) 1713.
[4] J.H. Harris et al., Proc. 22th EPS Conf. Plasma Phys. 19c (1995) IV-397.
[5] X. Litaudon et al., Nucl. Fusion 32 (1992) 1883.
[6] P.C. Stangeby, J. Nucl. Mater. 128–129 (1984) 969.
[7] J.-M. Noterdaeme and G. Van Oost, Plasma Phys. Controlled Fusion 35 (1993) 1481.
[8] M. Goniche et al., Proc. 23th EPS Conf. Plasma Phys. (1996), to be published.
[9] B.V. Chirikov, Phys. Rep. 52 (1979) 263.
[10] V. Fuchs et al., Phys. Plasmas, to be published.